SUPPLEMENTAL MATERIAL FOR:

Concurrent extreme events of atmospheric moisture transport and continental precipitation: the role of landfalling atmospheric rivers

Luis Gimeno-Sotelo [a,*] , Luis Gimeno [a]

[a] *Centro de Investigación Mariña, Universidade de Vigo, Environmental Physics Laboratory (EPhysLab), Ourense, Spain*
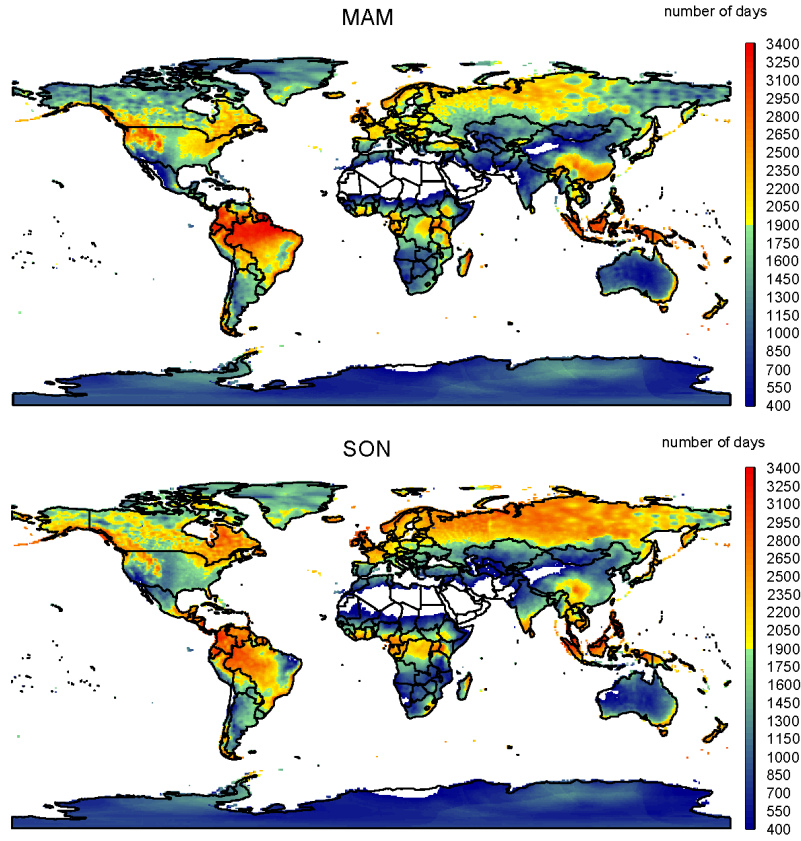[*] *Corresponding author (luis.gimeno-sotelo@uvigo.es)*

Figure S1: Total number of days for the period 1981-2017 with non-zero precipitation at each grid point for March-April-May (top) and September-October-November (bottom).
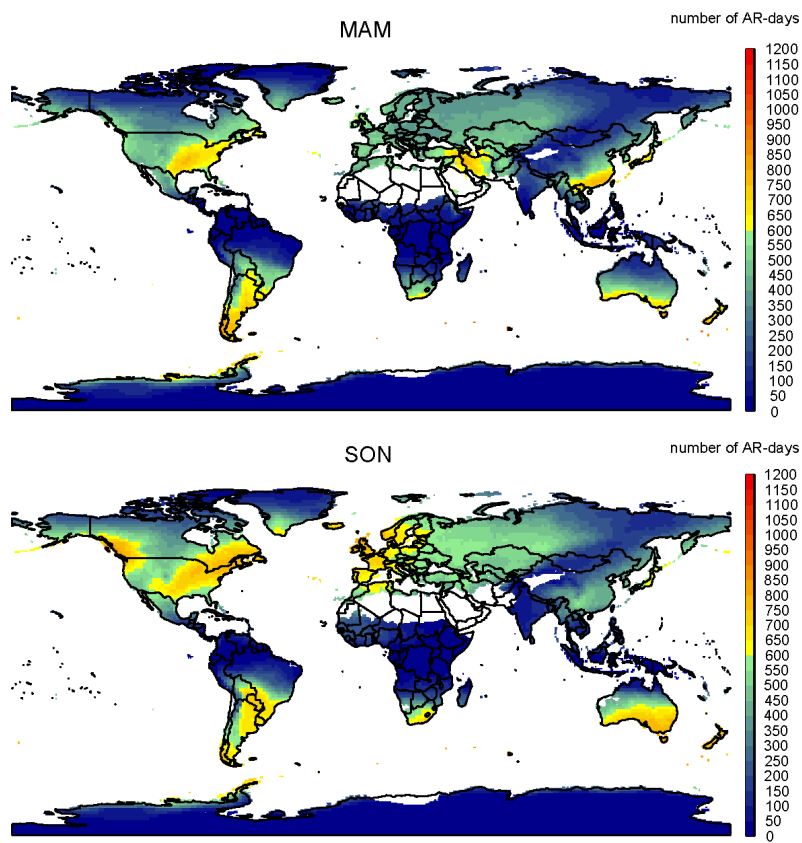
Figure S2: Number of days of occurrence of landfalling ARs for the period 1981-2017 at each grid point, for March-April-May (top) and September-October-November (bottom).
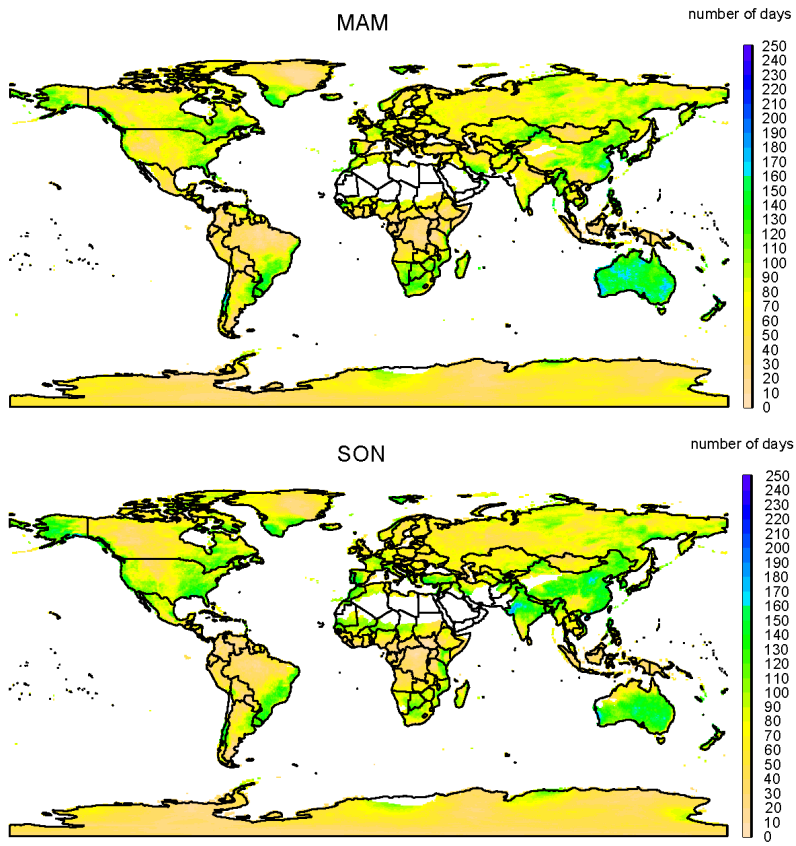
Figure S3: Number of days exceeding the bivariate threshold ($q90_{IVT}$, $q90_{prec}$) for March-April-May (top) and September-October-November (bottom) for the period 1981-2017.
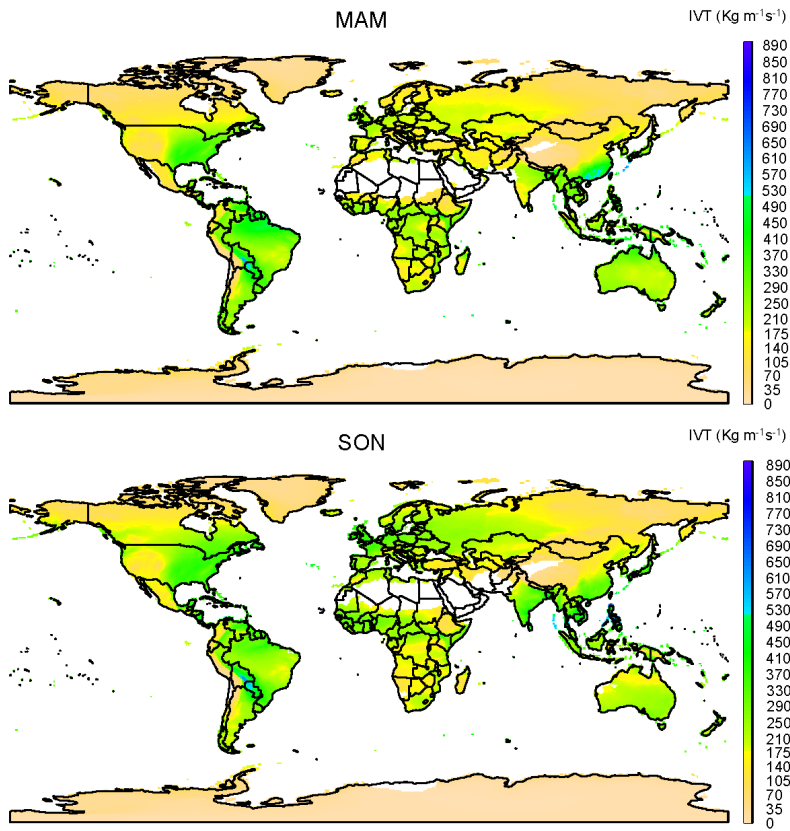
Figure S4: 90th percentile of IVT for March-April-May (top) and September-October-November (bottom) for the period 1981-2017.
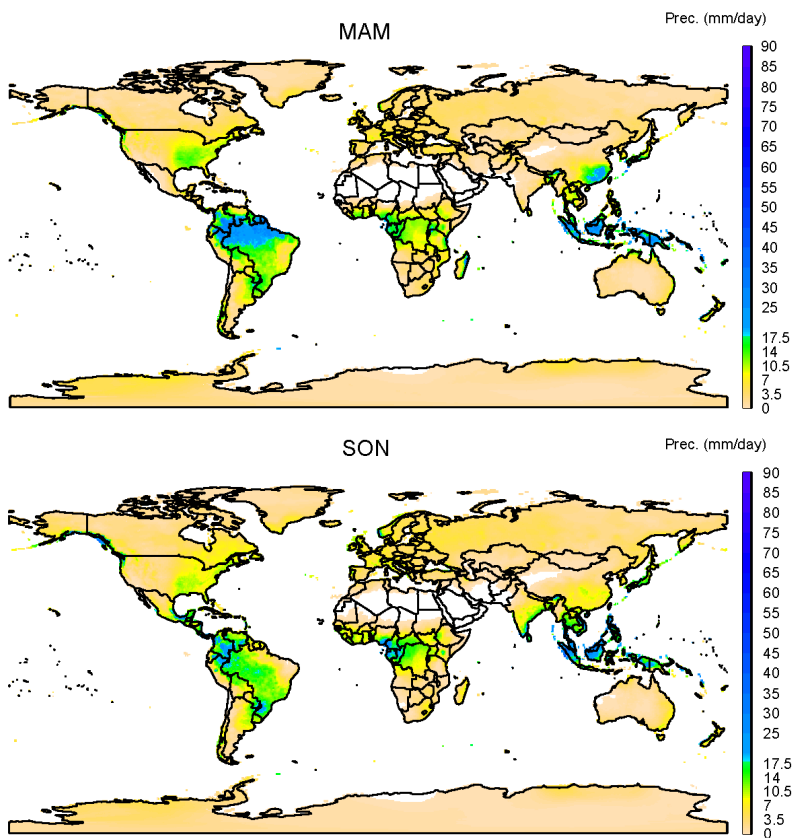
Figure S5: 90th percentile of continental precipitation for March-April-May (top) and September-October-November (bottom) for the period 1981-2017.
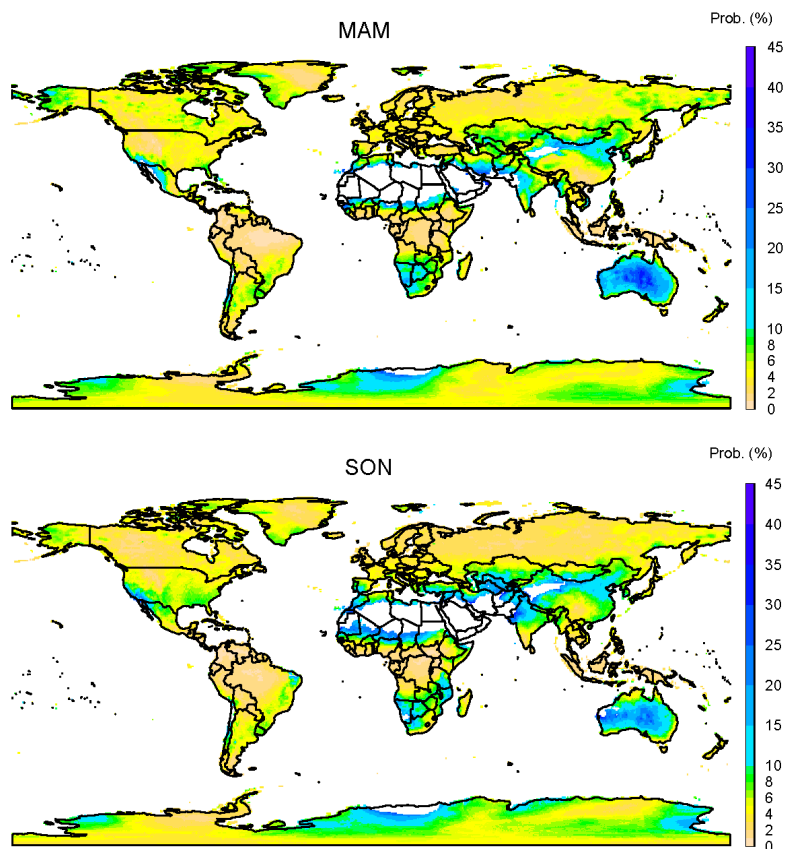
Figure S6: Estimated probability of achieving a concurrent extreme of IVT and continental precipitation (percent), for March-April-May and September-October-November for the period 1981-2017. It is computed using the copula model with the lowest AIC value for each grid point.

Whole period

MAM
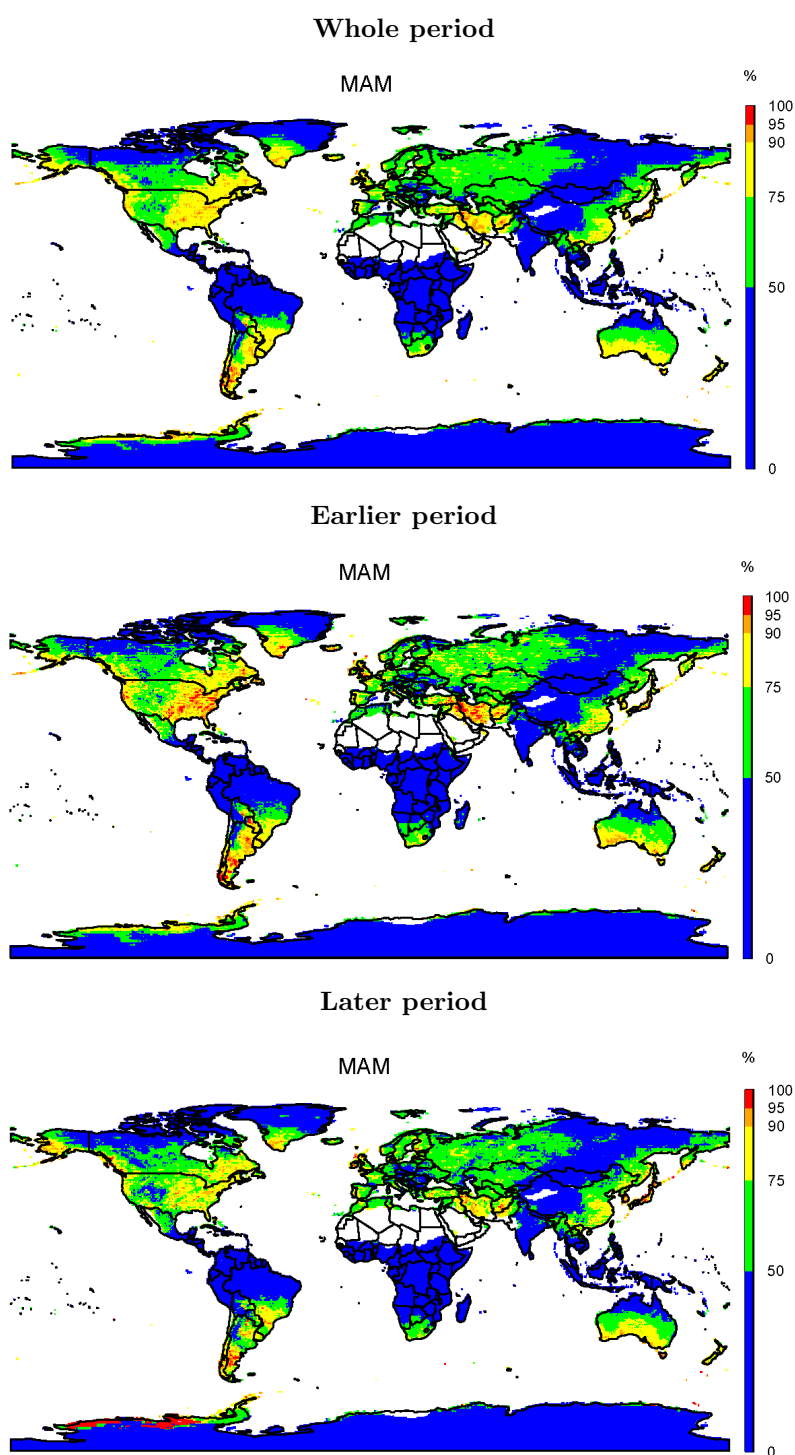

Earlier period

MAM

Later period

MAM

Figure S7: Percentage of concurrent extreme days of IVT and continental precipitation that coincide with the occurrence of landfalling ARs, for **March-April-May**, for the whole period 1981-2017, and the earlier and later studied periods.

Whole period

SON
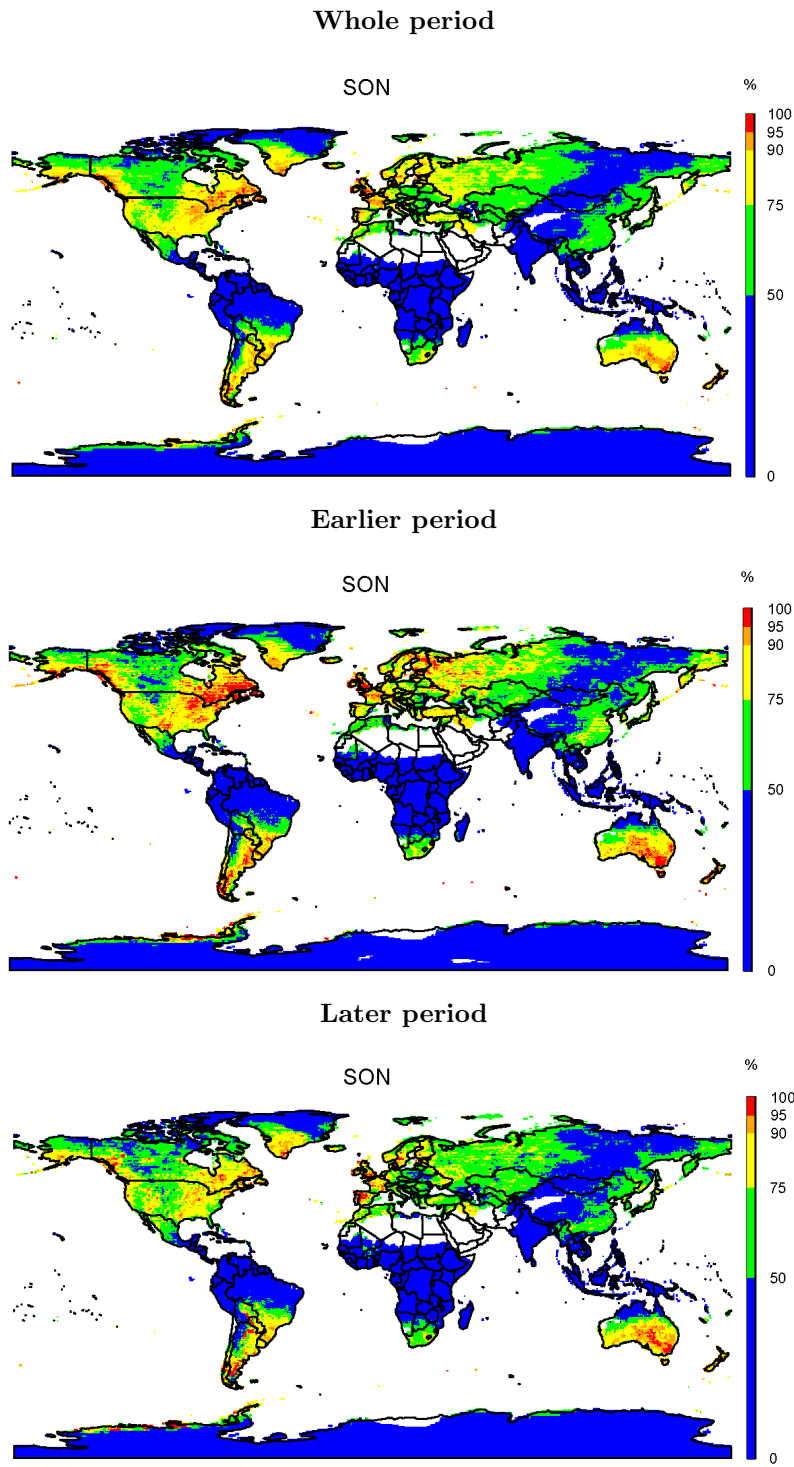

Earlier period

SON

Later period

SON

Figure S8: Percentage of concurrent extreme days of IVT and continental precipitation that coincide with the occurrence of landfalling ARs, for **September-October-November**, for the whole period 1981-2017, and the earlier and later studied periods.
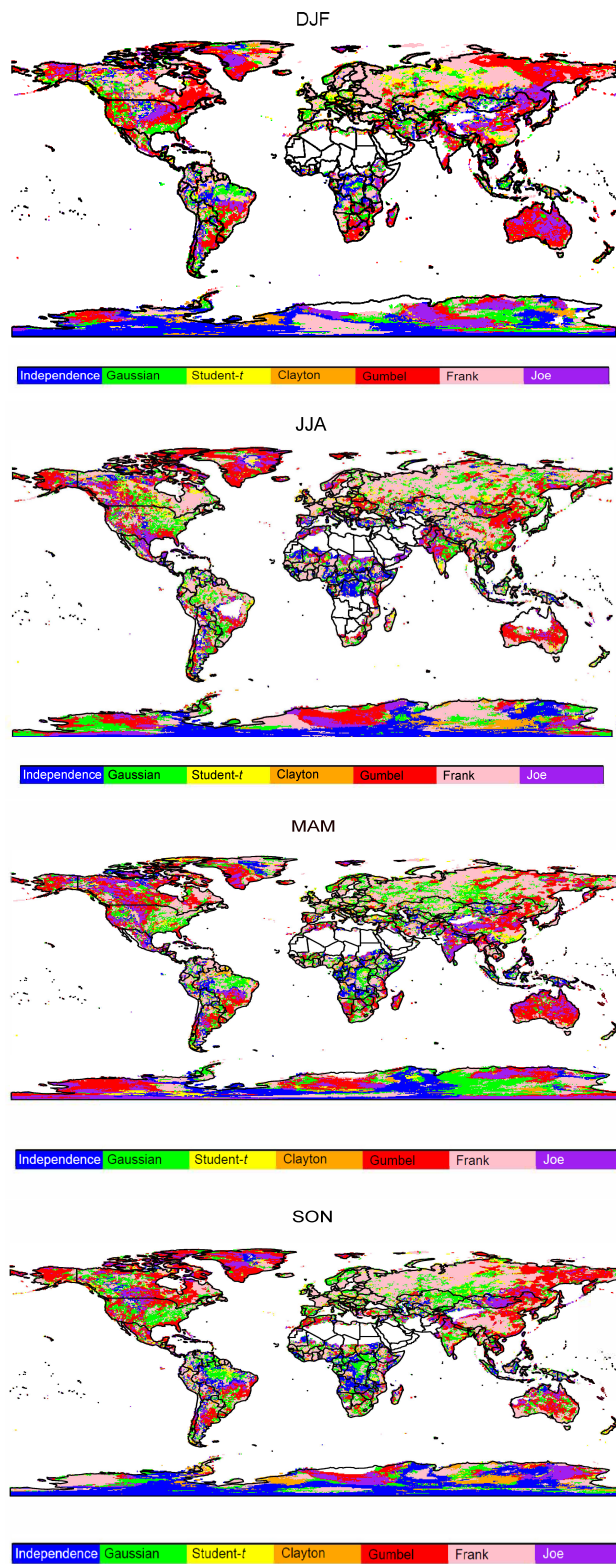
Figure S9: Fitted copula type with the lowest AIC value for each season for the period 1981-2017.